SAND2020-7494C

The Single-Volume Scatter Camera

Juan J. Manfredi[a], Evan Adamek[b], Joshua A. Brown[a], Erik Brubaker[c], Belkis Cabrera-Palmer[c], Joshua Cates[d], Ryan Dorrill[b], Andrew Druetzler[b], Jeff Elam[e], Patrick L. Feng[c], Micah Folsom[f], Aline Galindo-Tellez[b], Bethany L. Goldblum[a], Paul Hausladen[f], Nathan Kaneshige[b], Kevin Keefe[b], Thibault A. Laplace[a], John G. Learned[b], Anil Mane[e], Peter Marleau[c], John Mattingly[g], Mudit Mishra[g], Ahmed Moustafa[g], Jason Nattress[f], Kurtis Nishimura[b], John Steele[c], Melinda Sweany[c], Kyle Weinfurther[g], and Klaus-Peter Ziock[f]

[a]University of California, Berkeley, CA, USA 94720
[b]University of Hawai'i at Manoa, Honolulu, HI, USA 96822
[c]Sandia National Laboratory, Livermore, CA, USA 94550
[d]Lawrence Berkeley National Laboratory, Berkeley, CA, USA 94720
[e]Argonne National Laboratory, Lemont, IL, USA 60439
[f]Oak Ridge National Laboratory, Oak Ridge, TN, USA 37831
[g]North Carolina State University, Raleigh, NC, USA 27695

ABSTRACT

The multi-institution Single-Volume Scatter Camera (SVSC) collaboration led by Sandia National Laboratories (SNL) is developing a compact, high-efficiency double-scatter neutron imaging system. Kinematic emission imaging of fission-energy neutrons can be used to detect, locate, and spatially characterize special nuclear material. Neutron-scatter cameras, analogous to Compton imagers for gamma ray detection, have a wide field of view, good event-by-event angular resolution, and spectral sensitivity. Existing systems, however, suffer from large size and/or poor efficiency. We are developing high-efficiency scatter cameras with small form factors by detecting both neutron scatters in a compact active volume. This effort requires development and characterization of individual system components, namely fast organic scintillators, photodetectors, electronics, and reconstruction algorithms. In this presentation, we will focus on characterization measurements of several SVSC candidate scintillators. The SVSC collaboration is investigating two system concepts: the monolithic design in which isotropically emitted photons are detected on the sides of the volume, and the optically segmented design in which scintillation light is channeled along scintillator bars to segmented photodetector readout. For each of these approaches, we will describe the construction and performance of prototype systems. We will conclude by summarizing lessons learned, comparing and contrasting the two system designs, and outlining plans for the next iteration of prototype design and construction.

Keywords: Single Volume Scatter Camera, Neutron scatter camera, Organic scintillators, Neutron imaging, Proton light yield, Scintillator characterization, Neutron detection, Nuclear nonproliferation

1. INTRODUCTION

Kinematic neutron imaging is an established technique for characterizing fast-neutron radiation sources.[1–5] The principle is straightforward: detecting two successive neutron-proton elastic scatters (np-scatters) allows for the reconstruction of the incoming neutron energy and trajectory through the application of energy and momentum conservation. Modern systems are difficult to deploy and suffer from low efficiency of detecting double-scatter events. The Single Volume Scatter Camera (SVSC) project led by Sandia National Laboratories seeks to distinguish multiple np-scatters within a single organic-scintillator volume.[6] There are two important benefits to this approach. First, an order of magnitude decrease in the form factor compared to state-of-the-art cameras allows for significantly enhanced portability. Second, maximal acceptance of double-scatter events results in an

Further author information:
J.J.M.: E-mail: manfredi@berkeley.edu

estimated order of magnitude increase in detection efficiency. Together, these advantages can enable passive neutron imaging to be practically used in the field.

Figure 1 shows an illustration of the SVSC concept. An incoming neutron with energy E_n enters a single volume of organic scintillator and successively scatters elastically off of two protons. The energy of the neutron after the first np-scatter, $E_n^{'}$, can be determined using the distance (d_{10}) and time (t_{10}) between the two scatters:

$$E_n^{'} = \frac{1}{2} m_n \left(\frac{d_{10}}{t_{10}}\right)^2, \tag{1}$$

where m_n is the mass of the neutron. Because we are primarily concerned with fission-spectrum neutrons, this calculation is non-relativistic. By conservation of energy, the incoming neutron energy is given by

$$E_n = E_n^{'} + E_p, \tag{2}$$

where E_p is the energy of the recoiling proton from the first np-scatter. The proton light yield (PLY) of the scintillator material is needed in order to determine E_p, as the PLY relates scintillation light (which is measured by the photodetectors) to the energy of the recoiling proton. The scattering angle θ of the incoming neutron can be calculated from

$$\theta = \arccos\left(\sqrt{\frac{E_n^{'}}{E_n}}\right) = \arctan\left(\sqrt{\frac{E_p}{E_n}}\right), \tag{3}$$

and defines a cone of possible incoming neutron trajectories.

Multiple different SVSC prototypes are currently being designed and tested. These systems will be described in Section 2.

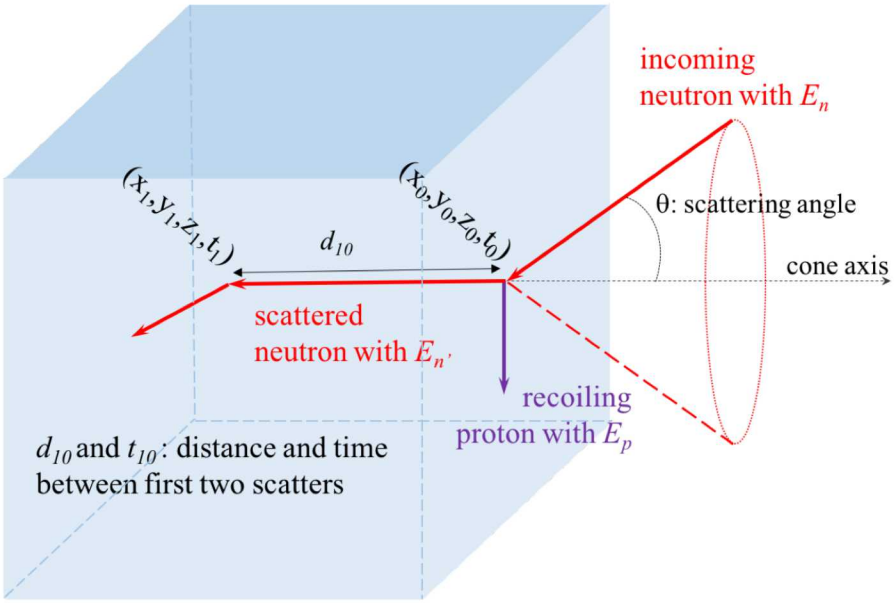

Figure 1: Diagram of kinematic neutron imaging within a single scintillator volume. An incoming neutron (with energy E_n) elastically scatters with a proton at location (x_0, y_0, z_0) and time t_0. The proton recoils with energy E_p. The scattered neutron interacts again with another proton within the scintillator volume at location (x_1, y_1, z_1) and time t_1. Using the distance (d_{10}) and the time (t_{10}) in between the two np-scatters, the scattered neutron energy can be calculated. The incoming neutron energy and the original scattering angle θ can then be reconstructed using the scattered neutron energy and the recoil proton energy from the first interaction.

To achieve the stated order-of-magnitude increase in double-scatter detection efficiency, the SVSC relies on the ability to resolve two separate proton recoils within a single scintillation volume. Accomplishing this task

requires determination of the energy of the scattered neutron to a precision similar to that of the recoil proton. For scatters of fission-spectrum neutrons separated by 10 cm, this corresponds to spatial and temporal resolutions of approximately 1 cm and 1 ns, respectively. Such resolutions represent a significant technical challenge. For this reason, the SVSC project includes several component-level research efforts, including the development of a high-channel-density electronics board,[7] performance evaluation of a Large Area Picosecond Photodetector, and frequency domain multiplexing of electronic signals.[8,9] These proceedings will describe in detail one such component research area in Section 3: scintillator characterization studies led by the University of California, Berkeley (UCB).

2. DESIGN CONCEPTS

2.1 Monolithic

The monolithic SVSC design consists of a single contiguous scintillator volume with photodetectors at the boundaries. The arrival times and positions of individual optical photons are detected, and photons are assumed to propogate isotropically from the location of the recoiling particle. Neutron-scatter events are reconstructed using a maximum likelihood approach which determines the event parameters most likely to yield the detected photon information. The likelihood is given by

$$\mathcal{L} = \frac{e^{-\mu}\mu^n}{n!}\prod_{i=1}^{n}\sum_{j=1}^{N}\frac{\mu_j}{\mu}P_{ji}, \tag{4}$$

where μ_j is the number of detected photons for the jth interaction (with $\mu = \sum \mu_j$), n is the number of detected photons, N is the number of neutron interactions in the event, and P_{ji} is the probability that the ith detected photon originates from the jth interaction. This probability can be expressed in terms of the times of emission (t_j) and detection (t_i) of photons, and the distance $d_{jk(i)}$ between the ith photon generated from the jth interaction and detected at the kth photodetector pixel:

$$P_{ji} = \frac{\frac{\Omega_{jk(i)}}{4\pi}Q_k e^{\frac{-d_{jk(i)}}{\lambda}} f\left(t_i - t_j - \frac{d_{jk(i)}}{c_{med}}\right)}{\sum_{k=1}^{n_{anode}}\frac{\Omega_{jk(i)}}{4\pi}Q_k e^{\frac{-d_{jk(i)}}{\lambda}}}, \tag{5}$$

where $f(t)$ is the scintillation pulse shape, $\Omega_{jk(i)}$ represents the solid-angle coverage of a specific interaction-pixel pair, and Q_k is the photodetection efficiency of the kth pixel. A proof-of-principle study showed that, given appropriate knowledge of the arrival times and positions of scintillation photons at the surface of the detector, it is possible to reconstruct the positions, times, and emitted light of proton recoils with sufficient accuracy for imaging by maximizing the log likelihood.[6]

A prototype has been constructed at Oak Ridge National Laboratory (ORNL) to experimentally demonstrate the monolithic concept. The prototype consists of a 5 cm x 5 cm x 5 cm cube of EJ-204 scintillator read out by two Hamamatsu H12700 64-anode PMTs on opposing sides of the cube, and to minimize reflections, the remaining four surfaces of the cube were painted black. The PMT anode signals were digitized using four CAEN V1742 32-channel waveform digitizers with a sampling rate of 5 GS/s. Figure 2 (left) shows a photograph of the assembled prototype.

In order to reconstruct neutron scattering interactions, best estimates of arrival times of individual photons had to be extracted from the PMT signals. To accomplish this, calibration of the response of each PMT anode was required to determine its quantum efficiency, gain, and timing offset. These calibrations were performed by sequentially presenting the attenuated output of a Photek LPG-405 picosecond laser via an optical fiber to each pixel of the PMTs and measuring the average number, pulse height, and times of detected photoelectrons. This process worked best when attenuation of the laser was such that the average number of detected photoelectrons was between 1 and 2.

For the present application, where many PMT anodes are illuminated simultaneously, crosstalk between anodes proved to be a major source of noise. While crosstalk between any pair of anodes is low (~2%), the

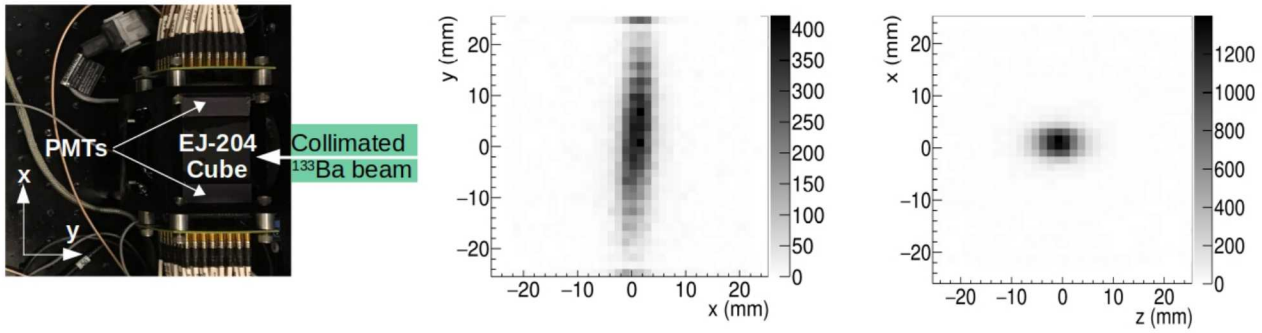

Figure 2: (Left) a photograph of the prototype detector and (right) spatial histograms of reconstructed positions of interactions of Compton-scattered gammas from a collimated ^{133}Ba source.

amplitude of the induced signal in one anode from the other 63 anodes can be larger than true signal. To address this problem, an iterative approach that uses an estimate of crosstalk from the average induced waveform was developed to extract the best estimate of true amplitudes and times of photoelectrons. This process increases the uncertainty in the pulse height and arrival time of single photoelectrons by about a factor of $\sqrt{2}$.

The position response of the prototype was evaluated by scanning the detector using collimated gamma-ray and neutron beams. An example of the reconstructed positions of interactions in the detector from of a collimated beam of gamma rays from a ^{133}Ba source is shown in Figure 2 (right). At present, reconstruction of single interaction locations has been demonstrated, but the reconstruction erroneously places the interactions toward the center of the detector. Further investigation identified that this systematic error originates from reflections off the PMTs modifying the probabilities P_{ji}. ORNL is presently working to pre-calculate and tabulate the P_{ji} via optical Monte-Carlo transport using Geant4.

Another prototype featuring direct reconstruction of scatter events was developed at ORNL in which optical photons pass through a coded aperture before detection.[10] This method introduces a high-frequency spatial component to the detected photon data, allowing for improved localization of neutron scatters within the scintillator volume. Simulation studies have shown the feasibility of this approach for a compact neutron-scatter camera, and were used to optimize the design of the prototype.

2.2 Optically Segmented

In the optically segmented (OS) SVSC approach, the detector volume is discretized into closely packed and optically isolated scintillator bars.[11] Each end of each bar is coupled to a silicon photomultiplier (SiPM), a low-cost and high-efficiency solid-state photodetector. Compared to the monolithic detector, the event reconstruction for the OS-SVSC is less technically challenging.

For each interation, the position along the bar (defined as the z-axis) is determined by comparing characteristics of the light observed at either end. There are two methods to perform this reconstruction. First, the difference in the arrival time of the scintillation pulse at the two ends can be expressed as

$$t_1 - t_2 = \frac{2z - L}{v}, \tag{6}$$

where L is the length of the bar, v is the velocity of light within the bar, and z is the position of the scintillation-light origin. The second reconstruction approach uses the log ratio of the amplitudes (A_1 and A_2) of the light pulses at either end of the bar. If the bulk attenuation of light in the scintillator can be described by an exponential with attenuation length λ, then the log ratio

$$\ln \frac{A_1}{A_2} = \frac{L - 2z}{\lambda}, \tag{7}$$

varies linearly with z. Both of these methods were tested through a series of single-bar characterization measurements with different organic scintillators and reflector materials.[12] EJ-204 wrapped in teflon yielded the best overall performance, and these results informed development of the prototype.

A first-generation OS prototype was constructed at the University of Hawai'i at Manoa. Figure 3 shows two photographs of the prototype. The system consists of 64 5 mm x 5 mm x 20 mm bars of EJ-204 (wrapped in teflon) in an 8 x 8 array, with each side coupled to an ArrayJ SiPM array from SensL. Pulses are digitized with custom electronics at a 1 GS/s rate and 12-bit resolution. System calibration and performance are currently in progress.

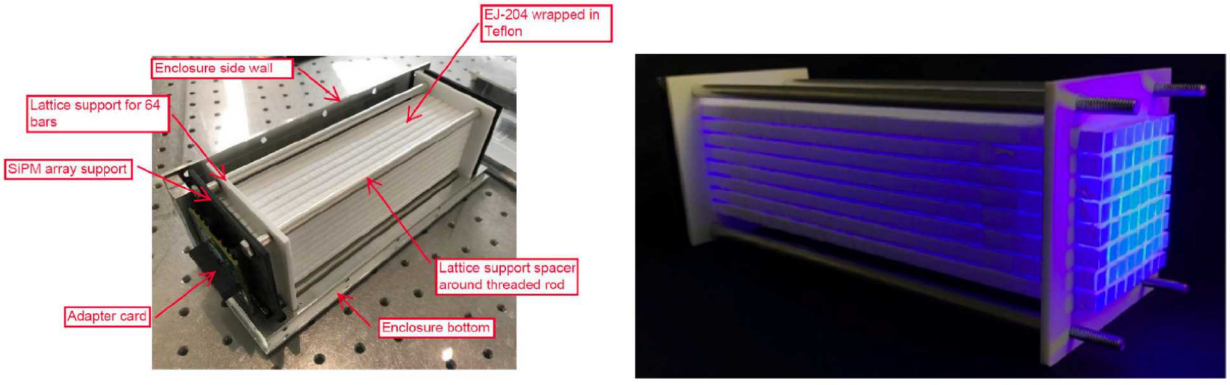

Figure 3: The OS-SVSC prototype at the University of Hawai'i at Manoa.

In addition, a second-generation prototype is under construction at Sandia National Laboratories in Livermore, California. The electronics for this prototype consist of a custom board with switched capacitor array chips that have a high sampling rate (5 GS/s) specifically designed for high fidelity timing measurements.[7] Like the first prototype, this system will have 64, EJ-204 scintillator bars. Rather than use commercially available SiPM arrays, we developed a custom interposer board with 16 SiPMs in a 2-by-8 configuration. This design allows for the full array of bars to be separated into constituent SiPM modules, enabling straightforward calibration using a gamma-ray source. The mechanical design for this system is complete. The electronics and interposer boards are being tested with a single-bar setup, after which the full array will be assembled.

3. SCINTILLATOR CHARACTERIZATION

Understanding properties of organic scintillator materials is vital to the design and operation of the SVSC. Light output, fast temporal response, particle discrimination, and robustness are all relevant considerations that impact imaging performance. Table 1 lists several scintillator materials under consideration for use within this project, as well as several relevant properties.

To inform SVSC system development, the team at UCB characterized the properties of candidate scintillator materials (including all those listed in Table 1) for the SVSC. A subset of these efforts are presented below.

3.1 Proton light yield for EJ-200, EJ-204 and EJ-208

As discussed in Section 1, kinematic neutron imaging relies on knowledge of the PLY of the scintillator, which is material-dependent and also nonlinear due to excitation quenching.[15] Measurements of the PLY for several candidate scintillators were performed at Lawrence Berkeley National Laboratory using the double-time-of-flight (dTOF) technique.[16] Deuterons are accelerated using the 88-Inch Cyclotron and impinge on a beryllium target, resulting in a high-flux, broad-spectrum neutron source. The scintillator of interest is placed in the neutron beam to induce np-scatters within the scintillator volume, and an array of pulse-shape discriminating scatter detectors are placed out of beam to measure the scattered neutrons. Using np-elastic scattering kinematics, this technique allows for an event-by-event measurement of the PLY.

Table 1: SVSC candidate organic scintillator materials and properties. For the materials from Eljen Technology, the listed properties (when available) are taken from the company website.[13] For the organic glass, the values are taken from a representative formulation.[14]

Scintillator material	Light output (% anthracene)	Rise time (ns)	Fall time (ns)	PSD
EJ-200	64	0.9	2.1	N
EJ-204	68	0.7	1.8	N
EJ-208	60	1.0	3.3	N
EJ-230	64	0.5	1.5	N
EJ-232	55	0.35	1.6	N
EJ-232Q	19	0.11	0.70	N
EJ-276	56	-	13	Y
Organic glass (G5)	112	-	1.45	Y

Many of the candidate materials for the SVSC are commercially available plastic scintillators from Eljen Technologies. In particular, a measurement of EJ-200, EJ-204, and EJ-208 was performed using the double-time-of-flight technique.[17] These materials all share the same polyvinyltoluene (PVT) primary base. The light output calibration was performed using relative light units (defined relative to the light from a 477 keV electron, corresponding to the Compton edge from the 662 keV gamma ray from ^{137}Cs) rather than electron-equivalent units. These units, although popular, inherently assume the proportionality of the electron light yield to electron recoil energy. Recent experimental evidence indicates that this assumption is not true in PVT-based scintillators,[18] which would render electron-equivalent units as poorly defined. The proton recoil energy was determined from the incoming neutron time-of-flight as well as the fixed scattering angles between the in-beam scintillator of interest and the EJ-309 scatter detectors. This approach results in a continuous measurement of the relationship between proton recoil energy and light output. The data were binned along the proton energy axis, and the projected light output histograms for each energy bin were fit using a maximum likelihood estimation considering a Gaussian peak and a piecewise power-law background. Systematic uncertainties were evaluated with a Monte Carlo-based approach, in which analysis parameters were varied within uncertainties and the resulting fluctuations in the final PLY were characterized.

Results for EJ-200, EJ-204, and EJ-208 are shown in Figure 4. The results are consistent between all three materials. In the case of EJ-204 (which is the scintillator used for both optically segmented and monolithic prototypes), the PLY measurement reaches a minimum proton recoil energy of 50 keV. Achieving a measurement with such a low energy is important for the SVSC, both because of the fission-spectrum neutron energies as well as the lack of a reliable physics-based scintillation model for extrapolation.

3.2 Proton light yield for EJ-230, EJ-232 and EJ-232Q

Several fast-plastic scintillators from Eljen (EJ-230, EJ-232, and EJ-232Q) were also measured with the dTOF technique.[19] The temporal characteristics of these materials make them attractive for use in the SVSC, where timing resolution is crucial for event reconstruction. Proton recoil energies were calculated using the scattering angle and the time-of-flight between the in-beam scintillator of interest and the relevant out-of-beam EJ-309 detector. Details of the calibration and analysis are otherwise similar to the previously described EJ-200/EJ-204/EJ-208 work. The resulting PLYs for EJ-230, EJ-232, and EJ-232Q are presented in Fig. 5, and agree within error. Furthermore, these PLYs are consistent with those measured with EJ-200, EJ-204, and EJ-208 scintillators. This is as expected because all six of these materials share the same PVT base, and ionization quenching is a primary process.[15]

In 2013, Enqvist, et al. observed an apparent change in the relative PLY of EJ-309 for different sized scintillator cells, and posited that this phenomenon was due to attenation of the scintillation light. To test this claim, we measured cylindrical scintillators of two different heights (2.54 cm and 5.08 cm) for both EJ-232 and

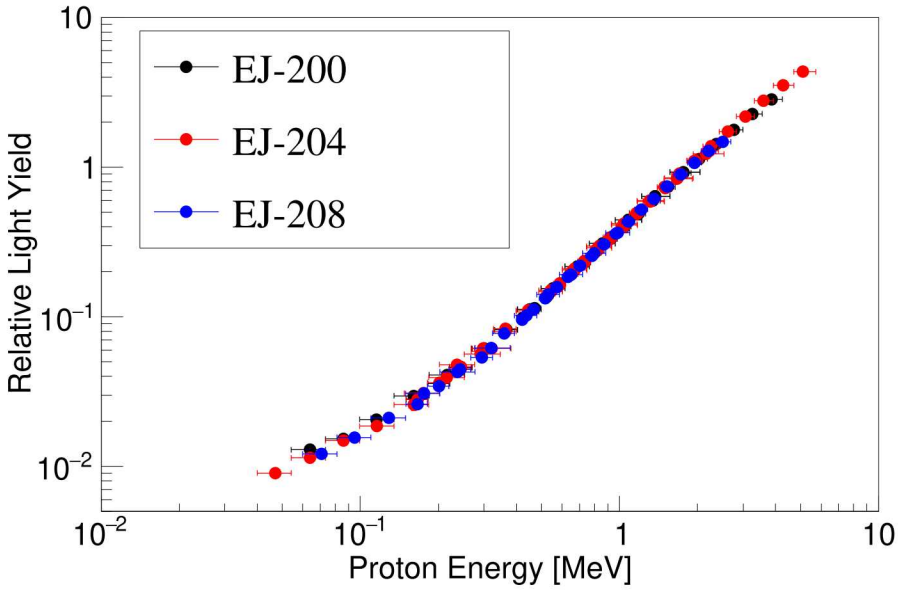

Figure 4: PLY measurements using the dTOF technique for EJ-200 (black), EJ-204 (red), and EJ-208 (blue).[17] The results are consistent within uncertainties across all three materials. The y-axis error bars indicate uncertainty from both statistical and systematic effects, while the x-axis error bars indicate the proton recoil energy bin sizes.

EJ-232Q. Both of these materials have significantly shorter attenuation lengths than EJ-309, so attenuation-based effects should be enhanced. Figure 6 shows the results for both EJ-232Q scintillators, which are consistent with each other within uncertainties. The EJ-232 measurements also indicated no evidence for scintillator size dependence.[19]

3.3 Novel organic glass

An optically transparent, melt-cast organic glass was developed by Carlson, et al. at SNL.[14,20] This organic glass material has high scintillation efficiency, pulse-shape discrimination (PSD) for identifying recoil particle type, and can be produced in high quantities at low cost. These properties make the organic glass a promising candidate for the SVSC. In particular, the PSD capability would allow for a powerful rejection of background gamma scatters from the double-neutron scatters of interest. Figure 7 shows a plot of the PSD metric (calculated for each event by taking the ratio of the tail integral of the digitized waveform to the full integral) as a function of light output. The neutron band and gamma bands are well separated down to approximately 0.2 relative light units.

We quantitatively evaluated the performance of the organic glass in comparison with two commercially available scintillator materials that also provide PSD: the liquid organic scintillator EJ-309, and the plastic organic scintillator EJ-276. The analysis is complete, and results will be published soon.

4. SUMMARY

The SVSC collaboration led by SNL is developing designs for a kinematic neutron scatter camera with an order-of-magnitude decrease in form factor and an order-of-magnitude increase in efficiency compared to state-of-the-art systems. Two prototype implementations are being pursued: a monolithic approach which features a single contiguous volume of scintillator and segmented photodetectors, and an optically segmented approach which consists of optically isolated scintillator bars coupled at either end to SiPMs. Detailed characteriztions of

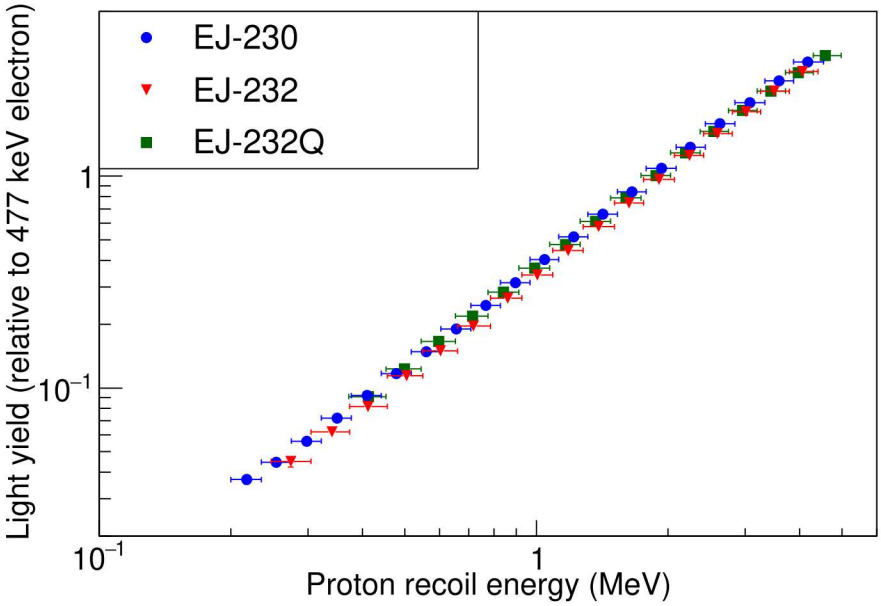

Figure 5: PLYs measurements using the dTOF technique for EJ-230 (blue circles), EJ-232 (red triangles), and EJ-232Q (green squares).[19] The results are consistent within uncertainties across all three materials. The y-axis error bars indicate uncertainty from both statistical and systematic effects, while the x-axis error bars indicate the proton recoil energy bin sizes. Reproduced with permission, copyright 2020, IEEE.[19]

these prototypes are currently underway, and lessons learned are being incorporated into subsequent prototypes. This project also supports several focused research and development efforts on individual system components, including electronics, scintillator materials, and photodetectors.

Scintillator characterization studies have been performed to better inform the design and development of the SVSC. The proton light yields of several candidate plastic scintillators (EJ-200, EJ-204, EJ-208, EJ-230, EJ-232, and EJ-232Q) were measured and, when possible, compared to existing literature values. We also investigated the claim that relative proton light yield depends on scintillator size by measuring two differently sized samples for both EJ-232 and EJ-232Q. No scintillator-size dependence was observed. A novel, pulse-shape discriminating organic glass designed by SNL is also a promising candidate for future systems. Other ongoing scintillator characterization projects include absolute light yield measurements, relative carbon light yield measurements, and the characterization of an organic plastic-glass scintillator developed at SNL.

ACKNOWLEDGMENTS

The authors thank the 88-Inch Cyclotron operations and facilities staff for their help in performing these experiments. Sandia National Laboratories is a multimission laboratory managed and operated by National Technology & Engineering Solutions of Sandia, LLC, a wholly owned subsidiary of Honeywell International Inc., for the U.S. Department of Energy's National Nuclear Security Administration under contract DE-NA0003525. The authors wish to thank the US DOE National Nuclear Security Administration, Office of Defense Nuclear Nonproliferation Research and Development for co-funding this work. Approved for unlimited release SANDXXXXX. This material is based upon work supported by the U.S. Department of Energy, National Nuclear Security Administration through the Nuclear Science and Security Consortium under Award DE-NA0003180 and Lawrence Berkeley National Laboratory under Contract DE-AC02-05CH11231. This paper describes objective technical results and analysis. Any subjective views or opinions that might be expressed in the paper do not necessarily represent the views of the U.S. Department of Energy or the United States Government.

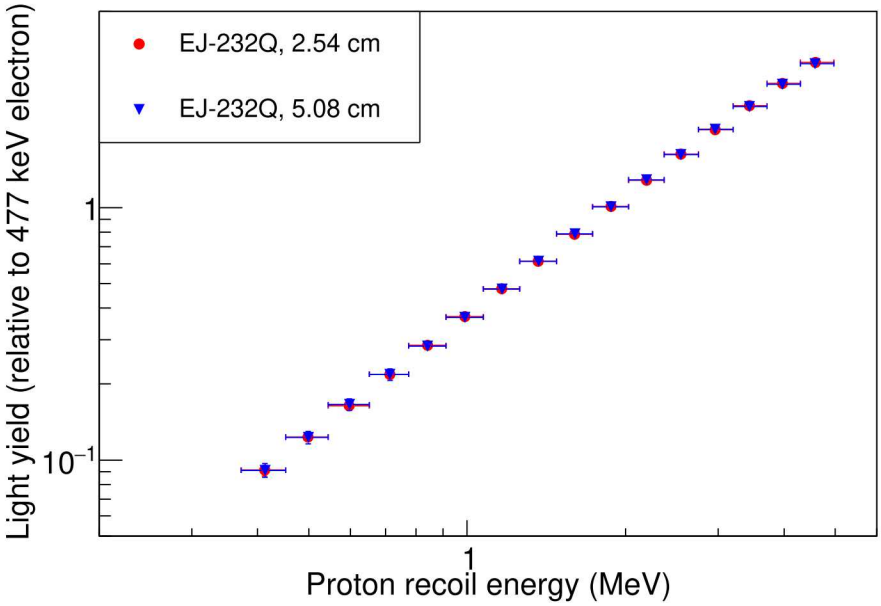

Figure 6: PLYs meausrements using the dTOF technique for two different EJ-232Q right-cylindrical, scintillators: one with a 2.54 cm height (red circles) and another with 5.08 cm height (blue triangles).[19] We observe no indication of size dependence in the PLY. The y-axis error bars indicate uncertainty from both statistical and systematic effects, while the x-axis error bars indicate the proton recoil energy bin sizes. Reproduced with permission, copyright 2020, IEEE.[19]

REFERENCES

[1] P. Marleau, J. Brennan, K. Krenz, N. Mascarenhas, and S. Mrowka, "Advances in imaging fission neutrons with a neutron scatter camera," in *2007 IEEE Nuclear Science Symposium Conference Record*, pp. 170–172, Institute of Electrical & Electronics Engineers (IEEE), oct 2007.

[2] N. Mascarenhas, J. Brennan, K. Krenz, P. Marleau, and S. Mrowka, "Results With the Neutron Scatter Camera," *IEEE Transactions on Nuclear Science* **56**, pp. 1269–1273, jun 2009.

[3] J. Brennan, E. Brubaker, R. Cooper, M. Gerling, C. Greenberg, P. Marleau, N. Mascarenhas, and S. Mrowka, "Measurement of the fast neutron energy spectrum of an ^{241}AmBe source using a neutron scatter camera," *IEEE Transactions on Nuclear Science* **58**, pp. 2426–2430, oct 2011.

[4] J. E. M. Goldsmith, M. D. Gerling, and J. S. Brennan, "A compact neutron scatter camera for field deployment," *Review of Scientific Instruments* **87**(8), p. 083307, 2016.

[5] W. M. Steinberger, M. L. Ruch, N. Giha, A. D. Fulvio, P. Marleau, S. D. Clarke, and S. A. Pozzi, "Imaging special nuclear material using a handheld dual particle imager," *Scientific Reports* **10**, Feb. 2020.

[6] J. Braverman, J. Brennan, E. Brubaker, B. Cabrera-Palmer, S. Czyz, P. Marleau, J. Mattingly, A. Nowack, J. Steele, M. Sweany, K. Weinfurther, and E. Woods, "Single-volume neutron scatter camera for high-efficiency neutron imaging and spectroscopy," *arXiv* , 2018.

[7] J. Steele, J. Brown, E. Brubaker, and K. Nishimura, "SCEMA: a high channel density electronics module for fast waveform capture," *Journal of Instrumentation* **14**, pp. P02031–P02031, feb 2019.

[8] M. Mishra, J. Mattingly, J. Mueller, and R. Kolbas, "Frequency domain multiplexing of pulse mode radiation detectors," *Nuclear Instruments and Methods in Physics Research Section A: Accelerators, Spectrometers, Detectors and Associated Equipment* **902**, pp. 117 – 122, 2018.

[9] M. Mishra, J. Mattingly, and R. Kolbas, "Application of deconvolution to recover frequency-domain multiplexed detector pulses," *Nuclear Instruments and Methods in Physics Research Section A: Accelerators, Spectrometers, Detectors and Associated Equipment* **929**, pp. 57 – 65, 2019.

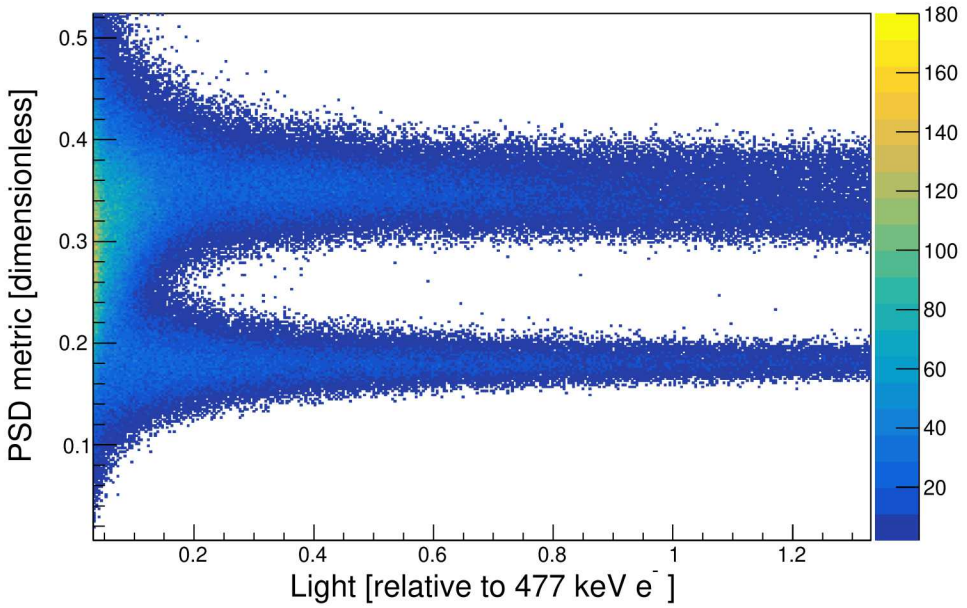

Figure 7: Pulse shape discrimination plot for the organic glass as a function of light. There is clear separation between the gamma band (bottom) and the neutron band (top) down to approximately 0.2 relative light units.

[10] M. J. Folsom, *A Compact Neutron Scatter Camera Using Optical Coded-Aperture Imaging*. PhD thesis, The University of Tennessee, Knoxville, May 2020.

[11] K. Weinfurther, J. Mattingly, E. Brubaker, and J. Steele, "Model-based design evaluation of a compact, high-efficiency neutron scatter camera," *Nuclear Instruments and Methods in Physics Research Section A: Accelerators, Spectrometers, Detectors and Associated Equipment* **883**, pp. 115–135, Mar. 2018.

[12] M. Sweany, A. Galindo-Tellez, J. Brown, E. Brubaker, R. Dorrill, A. Druetzler, N. Kaneshige, J. Learned, K. Nishimura, and W. Bae, "Interaction position, time, and energy resolution in organic scintillator bars with dual-ended readout," *Nuclear Instruments and Methods in Physics Research Section A: Accelerators, Spectrometers, Detectors and Associated Equipment* **927**, pp. 451 – 462, 2019.

[13] Eljen Technology, *Plastic Scintillators*, July 2020.

[14] J. S. Carlson, P. Marleau, R. A. Zarkesh, and P. L. Feng, "Taking advantage of disorder: Small-molecule organic glasses for radiation detection and particle discrimination," *Journal of the American Chemical Society* **139**(28), pp. 9621–9626, 2017. PMID: 28632383.

[15] J. Birks, *The Theory and Practice of Scintillation Counting*, ch. 8, pp. 269–320. Pergamon Press, 1964.

[16] J. A. Brown, B. L. Goldblum, T. A. Laplace, K. P. Harrig, L. A. Bernstein, D. L. Bleuel, W. Younes, D. Reyna, E. Brubaker, and P. Marleau, "Proton light yield in organic scintillators using a double time-of-flight technique," *Journal of Applied Physics* **124**(4), p. 045101, 2018.

[17] T. Laplace, B. Goldblum, J. Brown, D. Bleuel, C. Brand, G. Gabella, T. Jordan, C. Moore, N. Munshi, Z. Sweger, A. Sweet, and E. Brubaker, "Low energy light yield of fast plastic scintillators," *Nuclear Instruments and Methods in Physics Research Section A: Accelerators, Spectrometers, Detectors and Associated Equipment* **954**, p. 161444, 2020. Symposium on Radiation Measurements and Applications XVII.

[18] S. A. Payne, W. W. Moses, S. Sheets, L. Ahle, N. J. Cherepy, B. Sturm, S. Dazeley, G. Bizarri, and W. Choong, "Nonproportionality of scintillator detectors: Theory and experiment. ii," *IEEE Transactions on Nuclear Science* **58**(6), pp. 3392–3402, 2011.

[19] J. J. Manfredi, B. L. Goldblum, T. A. Laplace, G. Gabella, J. Gordon, A. OBrien, S. Chowdhury, J. A. Brown, and E. Brubaker, "Proton light yield of fast plastic scintillators for neutron imaging," *IEEE Transactions on Nuclear Science* **67**(2), pp. 434–442, 2020.

[20] J. S. Carlson and P. L. Feng, "Melt-cast organic glasses as high-efficiency fast neutron scintillators," *Nuclear Instruments and Methods in Physics Research Section A: Accelerators, Spectrometers, Detectors and Associated Equipment* **832**, pp. 152 – 157, 2016.